Supporting Information

Extraction of the intrinsic rate constant for a photocyclization reaction in capillary microreactors using a simplified reactor model

Jun Li, *[1&a] Helena Šimek Tosino, [&b] Bradley P. Ladewig,[c] Nicole Jung,[b,d] Stefan Bräse,[b,d] and Roland Dittmeyer [a]

[a] *Institute for Micro Process Engineering (IMVT), Karlsruhe Institute of Technology (KIT), Kaiserstraße 12, 76131 Karlsruhe, Germany*

[b] *Institute of Biological and Chemical Systems (IBCS-FMS), Karlsruhe Institute of Technology (KIT), Kaiserstraße 12, 76131 Karlsruhe, Germany*

[c] *Paul Wurth Chair in Energy Process Engineering Faculty of Science, Technology and Medicine, University of Luxembourg, Luxembourg*

[d] *Institute of Organic Chemistry (IOC), Karlsruhe Institute of Technology, Kaiserstraße 12, 76131 Karlsruhe, Germany*

* Corresponding author. E-mail address: jun.li@kit.edu
&These authors contributed to the work equally and should be regarded as co-first authors.

Test rig setup

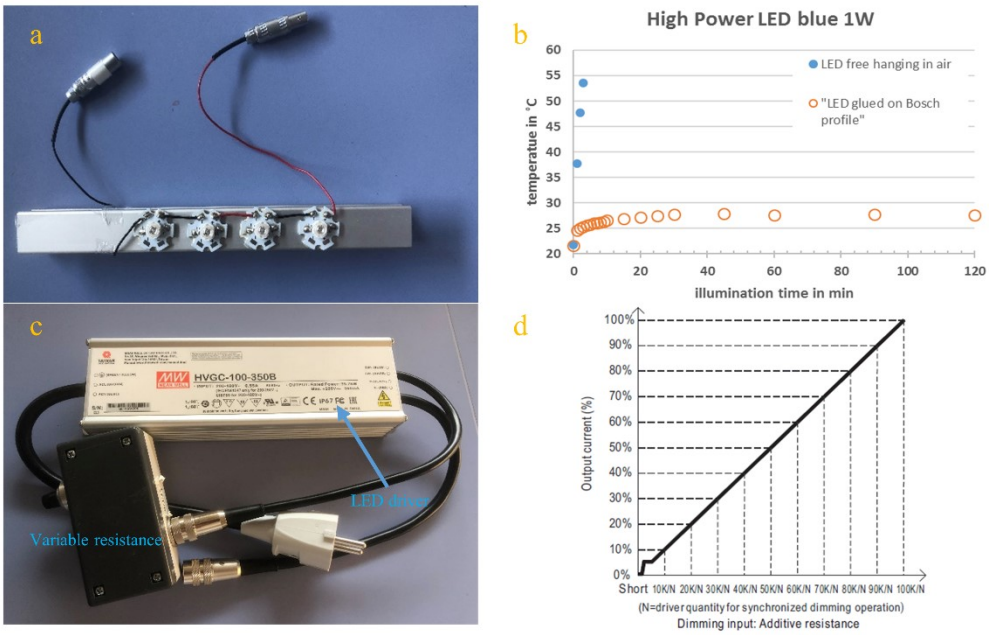

Figure S1 (a) LEDs glued on Bosch Profile (b) The plot of measured temperature versus illumination time (c) 100 W Meanwell constant current mode LED driver and variable external resistance (d) The plot of dimmable output current versus resistance, data from the manufacturer

Determination of photon flux in the capillary microreactor

Chemical actinometry

The classical potassium ferrioxalate actinometer (6 mM in 0.05 M sulfuric acid) with an estimated quantum yield Φ of 0.95 (from Fig. S4) at 465 nm was used in photon flux determination (Scheme S1). Eq. S1 shows the reaction rate expression of ferrioxalate photoconversion. The probability density function $p_{(\Omega)}$ can be further simplified as shown in Eq. S2-S3 for normal collimated and diffuse emission because the by-products are absorbing at shorter wavelength, and only the reactant gives contribution to the photon absorption.[1, 2]

$$2[Fe(C_2O_4)_3]^{3-} \xrightarrow{hv} 2Fe(C_2O_4) + 3[C_2O_4]^{2-} + 2CO_2$$

Scheme S1. Chemical actinometer used for characterization of photon flux in the microchannel

$$-\frac{dC_{act}}{dt} = \Phi\frac{q_\lambda}{V_R} \cdot p_{(\Omega)} \quad (1)$$

$$p_{(\Omega)} = \left[1 - \exp\left(-C_{act}E_{act,\lambda}L\right)\right] \quad (2)$$

$$p_{(\Omega)} = \left[1 + \exp(-C_{act}E_{act,\lambda}L)(C_{act}E_{act,\lambda}L - 1) + (C_{act}E_{act,\lambda}L)2Ei(-C_{act}E_{act,\lambda}L)\right] \quad (3)$$

where C_{act} stands for the used actinometer concentration and $E_{act,\lambda}$ stands for the napierian absorption coefficient of the actinometer for wavelength of interest. q_λ represents the amounts of photons absorbed in the reaction volume V_R=4 mL (einstein $\cdot$ s^{-1}). V_R corresponds to an internal volume of 4 mL for the microreactor. The value of $p_{(\Omega)}$ in Eq. S3 using 6 mM potassium ferrioxalate solution was returned by MATLAB 2019a with a value of **0.0672**.

The decomposition of ferrioxalate actinometer can be evaluated by complexation of the ferrous ions (Fe^{2+}) with o-phenanthroline whose strong absorbance appears at 510 nm. The resulting Fe^{2+} concentration can be derived from a calibration curve (Fig. S2) using an Agilent 8453 UV-Vis spectrophotometer. Steady-state operation was adopted in the photon flux determination of the PFA capillary microreactor: the solution was collected after 2.5 residence times (corresponding to a volume of 10 mL) elapsed. Detailed preparation and characterization procedures can be found somewhere else.[1, 3]

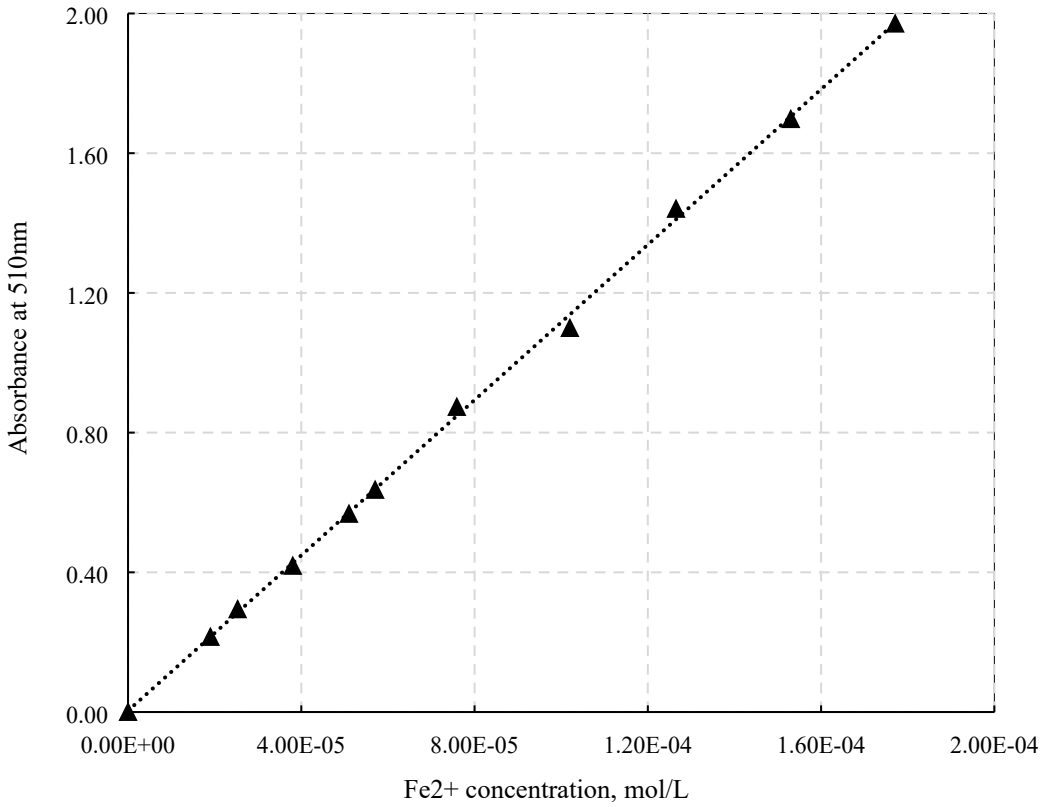

Figure S2 Calibration curve of ferrous ions (Fe^{2+})

Aillet et al. recommended that the decomposition of the actinometer should remain in low conversion (<10%) to get accurate results.[1] However, the conversions were high in our test rig even short residence times were adopted. The precipitation did not occur at low actinometer concentration and small fraction of CO_2 generated in the microchannel did not have strong influence on the results.[2] Following the recommendation from Shen *et al.*,[4] a second-order polynomial fitting was used to obtain the initial slope of the curve as initial reaction rate (Fig. S3). Fig. S4 shows the napierian absorption coefficient of the used potassium ferrioxalate and estimated quantum yield using six-order polynomial fitting versus wavelength of interest.[5] Therefore, this value was found to be 68.39 $L \cdot mol^{-1} \cdot cm^{-1}$ at 465 nm. The quantum yield for the used actinometer concentration (0.006 M in this case) was procured from the literature.[6] According to the conclusion from Radjagobalou *et al.*, the results from diffuse emission are more closed to true value.[7] To validate the strategy used here, the Reinecke's salt actinometer was also employed to determine the photon flux at 465 nm [2, 7-9]. Fig. S5 shows the fitting line

of the results using Reinecke's salt in the actinometer experiments. In addition, the value of $p_{(\Omega)}$ using 15 mM Reinecke's salt solution was returned by MATLAB 2019a with a value of **0.2423**. Table S1 lists the results on two different actinometers. It is clear that only small deviation can be observed for the weakest (40%) intensity. Therefore, the determination of the probability density function $p_{(\Omega)}$ using 1D Monte Carlo method is also applicable to a diluted concentration of ferrioxalate actinometer in the capillary microreactor. The results of incident photon flux of ferrioxalate actinometer were used in the main paper because less error was introduced by potassium ferrioxalate.

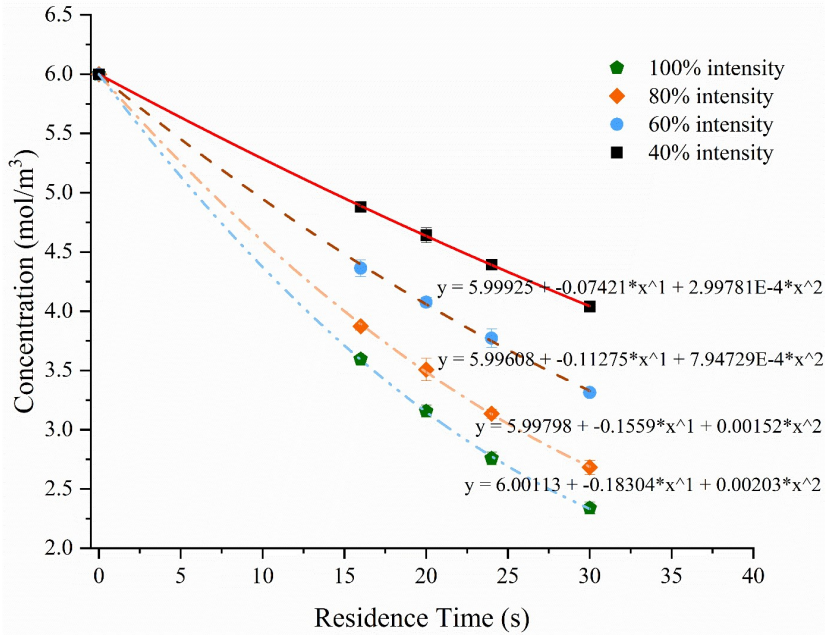

Figure S3 Concentration of the ferrioxalate actinometer versus residence time in the capillary microreactor at different light intensities using a 100W Meanwell constant current mode LED driver

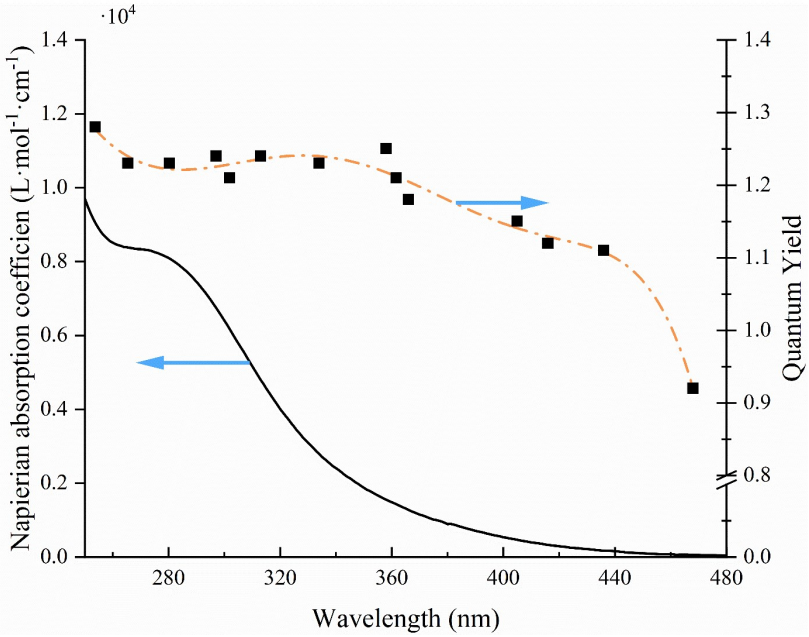

Figure S4 The plot of the Napierian absorption coefficient of $K_3[Fe(C_2O_4)_3]$ (solid line, derivated from 0.1 mM solution) and the estimated quantum yield of 0.006 M ferrioxalate over the investigated wavelength range (orange dash-dot line). Solid scatters were procured from reference.[6]

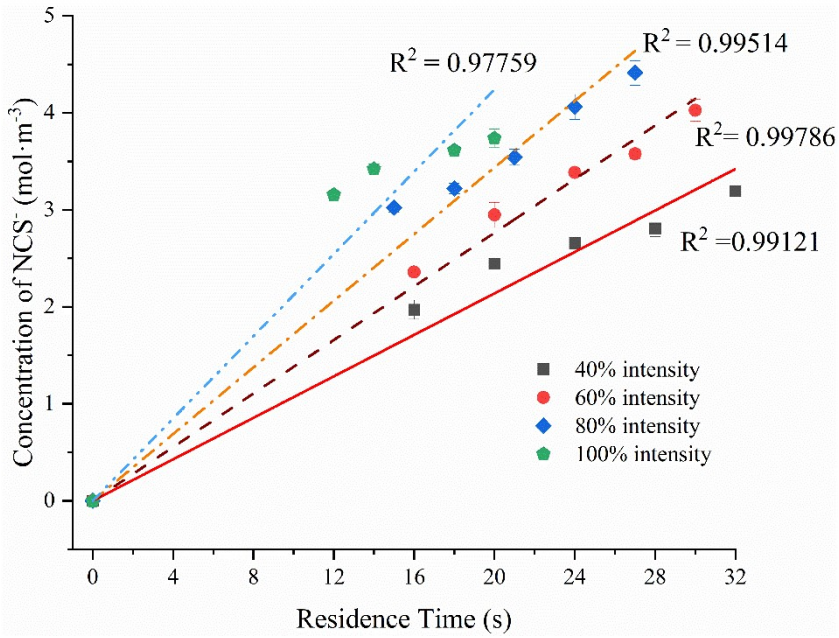

Figure S5 Plots of the concentration of NCS^- versus residence time in the capillary microreactor at different light intensities using a 100W Meanwell constant current mode LED driver

Table S1 Determining mean incident photon flux using ferrioxalate actinometer and Reinecke's salt actinometer

	Results from ferrioxalate			Results from Reinecke's salt		
Power	slope	$p_{(\Omega)}$	q_λ (einstein · s^{-1})	slope	$p_{(\Omega)}$	q_λ (einstein · s^{-1})
40%	-0.07421	0.0672	4.65E-06	0.10692	0.2423	5.86E-06
60%	-0.11275	0.0672	7.07E-06	0.13818	0.2423	7.58E-06

80%	-0.1559	0.0672	9.77E-06	0.17182	0.2423	9.42E-06
100%	-0.18304	0.0672	1.15E-05	0.21203	0.2423	1.16E-05

$p_{(\Omega)}$ was calculated by Eq. S3 with MATLAB R2019a.

Fig. S6 shows the UV-Vis spectrum of the iridium photocatalyst **2** at different concentration in anhydrous acetone and its calibration curve at 465 nm, the resulting slope in Fig. S6b represents its decimal molar attenuation coefficient. Likewise, the probability density function $p_{(\Omega)}$ of the iridium photocatalyst can be derived according to Eq. 8 in the main paper, assuming it is the only absorbing species and a value of **0.0591** was found. Table S2 summarises the results for the mean incident photon flux of diffuse emission over the capillary microreactor and the mean photon flux absorbed by the iridium photocatalyst.

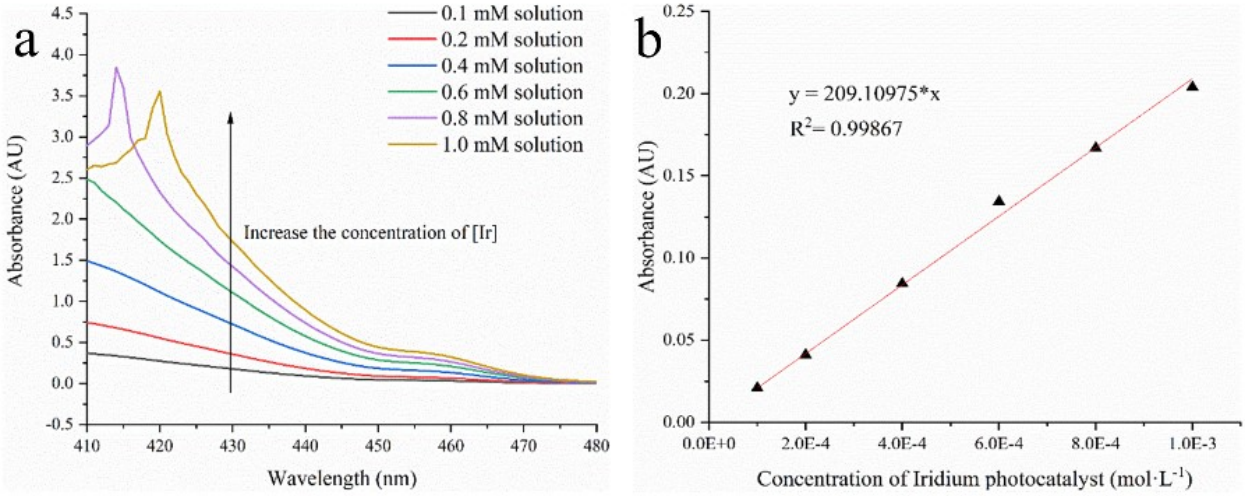

Figure S6 a) Calibration curves of the used iridium photocatalyst absorbance at 465 nm with its concentration in anhydrous acetone in a 10 mm path length cuvette. b) Extraction of the molar extinction coefficient of the used photocatalyst at 465 nm.

Table S2 Evaluation of incident photon flux of diffuse emission over the capillary microreactor and the mean absorbing photon flux by the used iridium photocatalyst **2**

Radiation Power	Incident photon flux (einstein.s^{-1})	Photon flux absorbed by the photocatalyst (einstein.s^{-1})
100%	1.15E-05	6.78E-07
80%	9.77E-06	5.78E-07
60%	7.07E-06	4.18E-07
40%	4.65E-06	2.75E-07

Photocyclization experiments

The flow experiments described below were based on the recently published batch photocyclization of the *o*-alkynylated *N*-alkyl-*N*-acylamide **1a** to the indole product **3a** under visible-light irradiation[10].

General procedure

N-Benzyl-2,2,3,3,4,4,5,5,6,6,7,7,8,8,8-pentadecafluoro-N-(2-(phenylethynyl)phenyl)octanamide (69.9 mg, 103 µmol, 1.00 equiv) and (Ir[dF(CF_3)ppy]$_2$(dtbpy))PF_6 (3.70 mg, 3.13 µmol, 0.0305 equiv) were dissolved in 4 mL of anhydrous acetone. The solution was transferred to a syringe and pumped through PFA tube via a syringe pump for respective time under irradiation with blue LED light of corresponding intensity (47.6 W, 38.1 W, 28.6 W, and 19.1 W for 100%, 80%, 60% and 40% of light intensity, respectively). The raw mixture was collected in a flask and acetone was evaporated under reduced pressure. After drying under high vacuum for 1 hour, NMR of the raw mixture was measured, and product-to-starting material ratio was determined. Reaction yield was calculated from this value. All experiments from this study were conducted on the same scale described in this general procedure.

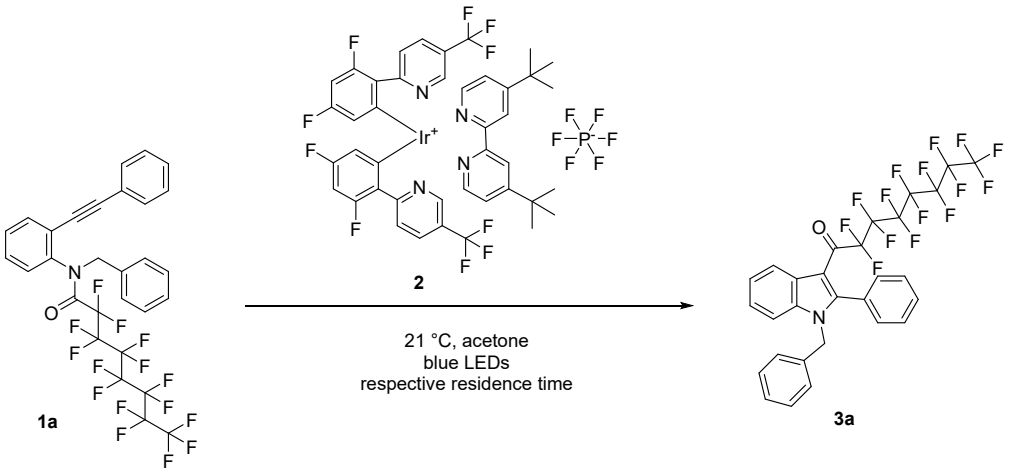

^{1}H NMR (400 MHz, $CDCl_3$ [7.26 ppm], ppm) δ = 8.14 (d, J = 8.1 Hz, 1H), 7.41–7.37 (m, 1H), 7.34–7.26 (m, 3H), 7.23–7.17 (m, 7H), 6.84–6.82 (m, 2H), 5.10 (s, 2H).

This product was also synthesized, purified and fully characterized in a batch experiment under optimized conditions available under: https://dx.doi.org/10.14272/reaction/SA-FUHFF-UHFFFADPSC-CDVMGELSTO-UHFFFADPSC-NUHFF-NUHFF-NUHFF-ZZZ.1

The ^{1}H analysis of the reaction product **3a** given above was extracted from this experiment.

Full analysis of the target product is available under: https://dx.doi.org/10.14272/reaction/SA-FUHFF-UHFFFADPSC-CDVMGELSTO-UHFFFADPSC-NUHFF-NUHFF-NUHFF-ZZZ

Experiments A: 100% light intensity (47.6 W)

This experiment was conducted according to the general procedure described above. The reaction mixture was irradiated with the blue light of 100% intensity (47.6 W) for reaction times ranging from 5 to 180 minutes and the results are summarized below:

Residence time, min	Product:starting material ratio	Yield, %
180	1:0.58	63.30
120	1:0.82	54.95
90	1:1.32	43.10
60	1:1.72	36.76
45	1:2.18	31.45
30	1:3.17	23.98
15	1:6.40	13.51
10	1:17.06	5.54
5	1:48.92	2.00

Additional information on the chemical synthesis is available via Chemotion repository: https://dx.doi.org/10.14272/reaction/SA-FUHFF-UHFFFADPSC-CDVMGELSTO-UHFFFADPSC-NUHFF-NUHFF-NUHFF-ZZZ.5

Additional information on the analysis of the target compound is available via Chemotion repository: https://dx.doi.org/10.14272/CDVMGELSTOUEQI-UHFFFAOYSA-N.5

Experiments B: 80% light intensity (38.1 W)

This experiment was conducted according to the general procedure described above. The reaction mixture was irradiated with the blue light of 80% intensity (38.1 W) for reaction times ranging from 5 to 180 minutes and the results are summarized below:

Residence time, min	Product:starting material ratio	Yield, %
180	1:0.76	56.82
120	1:1.08	48.10
90	1:1.4	40.90
60	1:2.00	33.33
45	1:3.20	23.81
30	1:3.84	20.66
15	1:8.58	10.44
10	1:22.4	4.27
5	1:80.0	1.24

Additional information on the chemical synthesis is available via Chemotion repository: https://dx.doi.org/10.14272/reaction/SA-FUHFF-UHFFFADPSC-CDVMGELSTO-UHFFFADPSC-NUHFF-NUHFF-NUHFF-ZZZ.4

Additional information on the analysis of the target compound is available via Chemotion repository: https://dx.doi.org/10.14272/CDVMGELSTOUEQI-UHFFFAOYSA-N.4

Experiments C: 60% light intensity (28.6 W)

This experiment was conducted according to the general procedure described above. The reaction mixture was irradiated with the blue light of 60% intensity (28.6 W) for reaction times ranging from 10 to 180 minutes and the results are summarized below:

Residence time, min	Product:starting material ratio	Yield, %
180	1:1.08	48.08
120	1:1.74	36.80
90	1:1.96	33.78
60	1:2.58	27.93
45	1:3.56	31.92
30	1:5.02	16.60
15	1:11.30	8.13
10	1:42.7	2.29

Additional information on the chemical synthesis is available via Chemotion repository: https://dx.doi.org/10.14272/reaction/SA-FUHFF-UHFFFADPSC-CDVMGELSTO-UHFFFADPSC-NUHFF-NUHFF-NUHFF-ZZZ.3

Additional information on the analysis of the target compound is available via Chemotion repository: https://dx.doi.org/10.14272/CDVMGELSTOUEQI-UHFFFAOYSA-N.3

Experiment D: 40% light intensity (19.1 W)

This experiment was conducted according to the general procedure described above. The reaction mixture was irradiated with the blue light of 40% intensity (19.1 W) for reaction times ranging from 10 to 180 minutes and the results are summarized below:

Residence time, min	Product:starting material ratio	Yield, %
180	1:1.62	38.17
120	1:2.40	29.41
90	1:2.74	26.73
60	1:3.84	20.66
45	1:5.16	16.23
30	1:9.78	9.28
15	1:54.1	1.81
10	1:74.42	1.33

Additional information on the chemical synthesis is available via Chemotion repository: https://dx.doi.org/10.14272/reaction/SA-FUHFF-UHFFFADPSC-CDVMGELSTO-UHFFFADPSC-NUHFF-NUHFF-NUHFF-ZZZ.2

Additional information on the analysis of the target compound is available via Chemotion repository: https://dx.doi.org/10.14272/CDVMGELSTOUEQI-UHFFFAOYSA-N.2

COMSOL simulation

Computational domain and meshing

Fig. S7 presents the simulative domain and meshing. The parametric sweep function was used in COMSOL Multiphysics for parallel computation to obtain stationary solutions of velocity fields of different residence times (15-180 min). Then, the resulting velocity fields were transferred for multiphysics coupling of chemistry, diluted species transport, and reacting flow for a transient study in COMSOL. A step function from 0-1 with a transition zone of 0.05 was adopted for smoothing the initial concentration at the inlet, and an integration function was used to calculate the molar flow rate of the indole product **3a** as a function of time at the outlet, thus the total moles of **3a** produced.

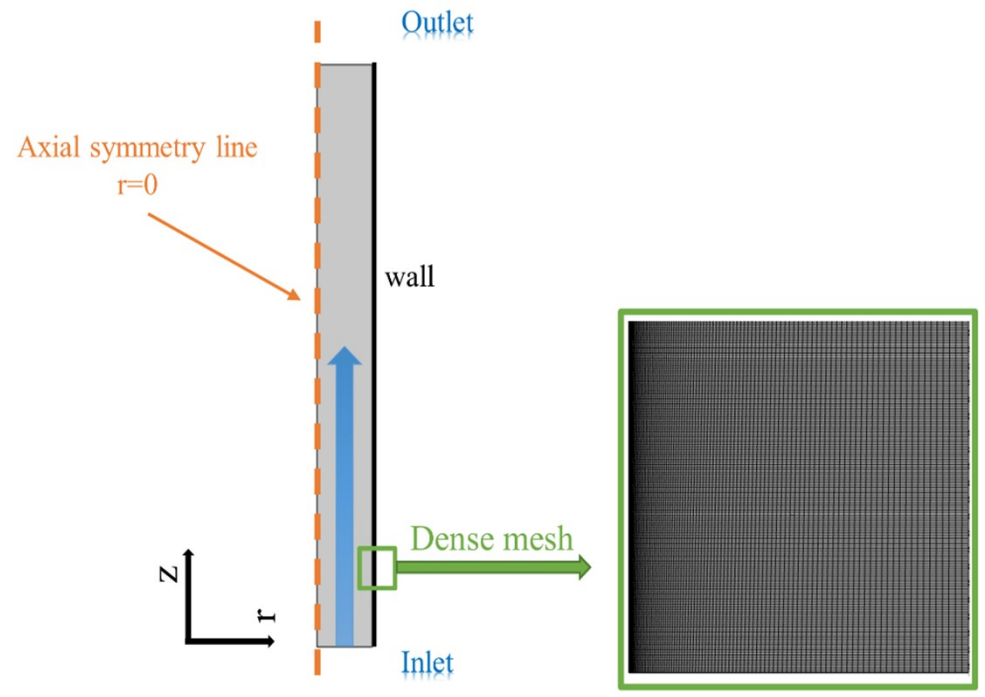

Figure S7 Schematic view of simulative domain and meshing. Employing dense grids near the wall in order to capture the boundary effects. Demo instruction is available on request.

Predicted moles of compound *3a* produced and estimated conversion by simulations

Table S3 Total moles of **3a** produced and estimated conversions from 2D axisymmetric numerical simulations

irradiation power	Mean hydrodynamic residence Time (min)	Total moles of **3a** produced	Estimated conversion (%)
100% output	15	12.29 µmol	12.29
	30	21.90 µmol	21.90
	45	29.64 µmol	29.64
	60	35.96 µmol	35.96
	90	45.68 µmol	45.68
	120	52.84 µmol	52.84
	150	58.34 µmol	58.34
	180	62.65 µmol	62.65
80% output	15	9.85 µmol	9.85
	30	18.19 µmol	18.19
	45	25.10 µmol	25.10
	60	30.90 µmol	30.90
	90	40.42 µmol	40.42
	120	47.57 µmol	47.57
	180	57.71 µmol	57.71
60% output	30	12.99 µmol	12.99
	45	18.43 µmol	18.43
	60	23.10 µmol	23.10
	90	31.20 µmol	31.20
	120	37.90 µmol	37.90
	180	47.86 µmol	47.86
40% output	30	9.78 µmol	9.78
	45	14.06 µmol	14.06
	60	17.93 µmol	17.93
	90	24.87 µmol	24.87
	120	30.68 µmol	30.68
	180	39.98 µmol	39.98

Comparison between experimental results and simulations

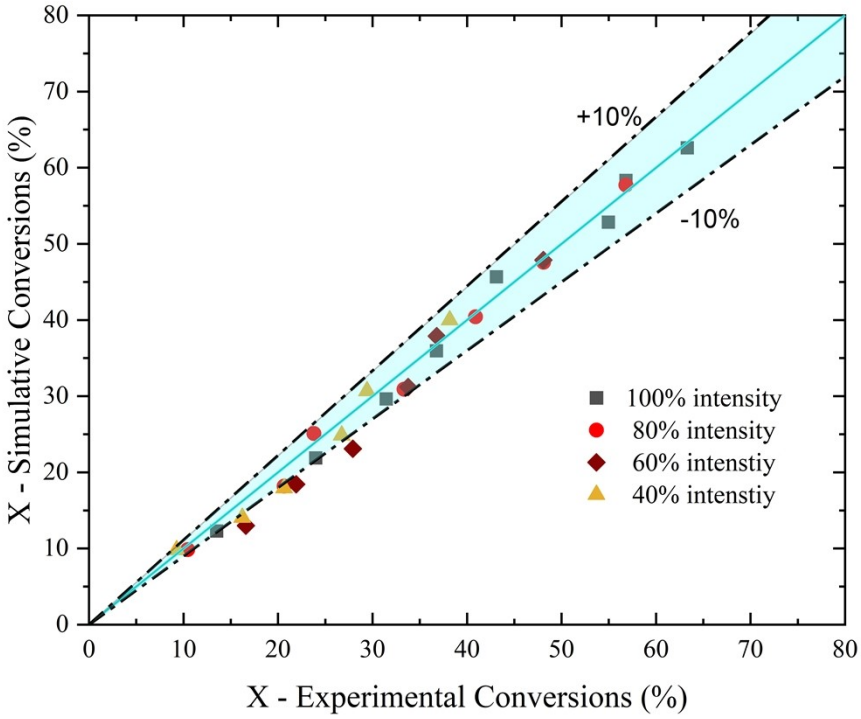

Figure S8 Polarity plot of experimental results and simulations for a mean hydrodynamic residence time of 15-180 minutes at different light intensities, simulation data refer to Table S3.

Parameters for simulation

Table S4 lists the input kinetics parameters for reactor simulations

Table S4 Key parameters for COMSOL simulation

Name	Expression	Description
L	V_R/(pi*D^2/4)	Length of PFA tubing
D	0.8[mm]	Inner radius of PFA tubing
D_{ref}	1E-9 [m^2/s]	Reference diffusivity for species
V_R	4 [cm^3]	Volume of illuminated area
K_app_100	0.3799 [L/(mol*min)]	Apparent rate constant 100% intensity
K_app_80	0.3123 [L/(mol*min)]	Apparent rate constant 80% intensity
K_app_60	0.2096 [L/(mol*min)]	Apparent rate constant 60% intensity
K_app_40	0.1519 [L/(mol*min)]	Apparent rate constant 40% intensity
rho_acetone	0.7844 [g/(cm^3)]	Density of acetone
mu_acetone	0.316[cP]	Dynamic viscosity of acetone
Q_in	4[cm^3]/t_res	Volumetric flow rate
cA_in	0.025 [M]	Inlet concentration of the reactant **1a**
cB_in	0 [M]	Inlet concentration of the product **3a**
Mn_r	679.419488 [g/mol]	Molar weight of the reactant **1a**
Mn_p	679.419488 [g/mol]	Molar weight of the product **3a**
Mn_Ir	1121.91 [g/mol]	Molar weight of the Iridium catalyst **2**
Mn_acetone	58.079140 [g/mol]	Molar weight of acetone
t_res	15-180[min]	Residence time

Reference

1. T. Aillet, K. Loubiere, O. Dechy-Cabaret and L. Prat, *Int J Chem React Eng*, 2014, **12**.
2. V. Rochatte, G. Dahi, A. Eskandari, J. Dauchet, F. Gros, M. Roudet and J. F. Cornet, *Chemical Engineering Journal*, 2017, **308**, 940-953.
3. C. G. Hatchard and C. A. Parker, *Proc R Soc Lon Ser-A*, 1956, **235**, 518-536.
4. C. Shen, M. Shang, H. Zhang and Y. Su, *AIChE Journal*, 2019, **66**.
5. B. Wriedt, D. Kowalczyk and D. Ziegenbalg, *Chemphotochem*, 2018, **2**, 913-921.
6. J. Rabani, H. Mamane, D. Pousty and J. R. Bolton, *Photochem Photobiol*, 2021, **97**, 873-902.
7. R. Radjagobalou, V. D. D. Freitas, J. F. Blanco, F. Gros, J. Dauchet, J. F. Cornet and K. Loubiere, *Journal of Flow Chemistry*, 2021, **11**, 357-367.
8. E. E. Wegner and A. W. Adamson, *Journal of the American Chemical Society*, 1966, **88**, 394-404.
9. R. Radjagobalou, J.-F. Blanco, V. Dias da Silva Freitas, C. Supplis, F. Gros, O. Dechy-Cabaret and K. Loubière, *Journal of Photochemistry and Photobiology A: Chemistry*, 2019, **382**, 111934.
10. H. Simek Tosino, A. Jung, O. Fuhr, C. Muhle-Goll, N. Jung and S. Bräse, *Eur J Org Chem*, 2023, **26**, e202201132.